

# Conservative Overset for Discontinuous Galerkin Methods

Steve Tran

June 1, 2021

## 1 Discontinuous Galerkin Formulation

The problem of interest is the 1D advection equation, shown below in its strong form.

$$u_{,t} + au_{,x} = 0 \quad (1)$$

where  $u$  is the unknown,  $a$  is the convection speed,  $x$  is space, and  $t$  is time. Note that Einsteinian index notation is used. Following the traditional finite element formulation, Equation (1) is multiplied by an arbitrary weighting function,  $w$ , and then is integrated over the domain. Using integration by parts, we arrive at (2).

$$\int_{\Omega} [wu_{,t} - aw_{,x}u] d\Omega + awu|_{\Gamma} = 0 \quad (2)$$

where  $\Omega$  represents the domain and  $\Gamma$  represents the boundaries of the domain. Following the finite element method, the domain is split up into a number of discrete 1D elements, described by Equation (3).

$$\int_{\Omega_e} [wu_{,t} - aw_{,x}u] d\Omega_e + awu|_{\Gamma_e} = 0 \quad (3)$$

Quantities with the subscript  $e$  denote elemental quantities. Next the weighting function and unknown variables are decomposed into the products of space-dependent shape functions and time-varying coefficients as follows:

$$w(x, t) = \sum_{i=1}^{nshp} N_i(x) \hat{w}(t) \quad (4)$$

$$u(x, t) = \sum_{i=1}^{nshp} N_i(x) \hat{u}(t) \quad (5)$$

where  $N(x)$  are the shape functions,  $nshp$  is the number of bases on any given element, and  $\hat{\cdot}$  denotes the variable coefficients. The weighting function and the unknown variable are assumed to occupy the same space so the same shape functions are used for both  $w$  and  $u$ , although the exact shape functions used are chosen by the user and may vary from code to code.

The above equations can be substituted into Equation (3) and, recognizing that the weighting functions are arbitrary and their coefficients may be factored out, we arrive at the following equation.

$$\int_{\Omega_e} [N_a N_b \hat{u}_{b,t} - a N_{a,x} N_b \hat{u}_b] d\Omega_e + a N_a N_b \hat{u}_b|_{\Gamma_e} = 0 \quad (6)$$

Note again that Einstein notation is used so repeated indicies imply a summation. Then rearranging we arrive at the final equation that the code will solve.

$$\hat{u}_{b,t} \int_{\Omega_e} N_a N_b d\Omega_e - \int_{\Omega_e} a N_{a,x} N_b \hat{u}_b d\Omega_e + a N_a N_b \hat{u}_b|_{\Gamma_e} = 0 \quad (7)$$

Observe that this represents a system of equations for each element. The first term in Equation (7), called the “mass matrix”, is a matrix of size  $nshp \times nshp$  whereas the second and third terms, the convective and flux terms, respectively, are vectors of length  $nshp$ .

Using the discontinuous Galerkin (DG) approach, there is no requirement for the values of  $u$  to be continuous across elements, as shown in Figurefig:dg. Thus, special care must be taken with the flux vector,  $a N_a N_b \hat{u}_b|_{\Gamma_e}$ , in order to approximate the inter-element fluxes. In this work, a simple upwinding approach is used.

$$a u|_{\Gamma_e} \approx 0.5(a(u_L + u_R) - |a|(u_R - u_L)) \quad (8)$$

where  $u_L$  and  $u_R$  represent the left and right states of  $u$  across the element boundaries.

The volume integral terms needed to compute the mass matrix and the convective terms are found using numerical quadrature. In this case, Gauss-Legendre quadrature was used. For the time integration, the explicit third order Runge Kutta scheme was applied.

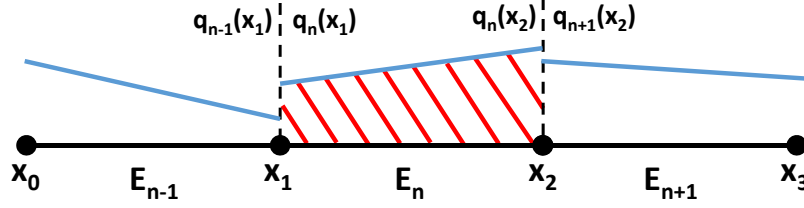


Figure 1: Schematic describing a conventional DG method on a single mesh, with fluxes calculated at the discontinuous boundaries and volume integrals calculated over the element (shown in striped red)

## 2 Overset Approach

Two methods are used to handle situations where the problem is solved on two or more separate but overlapping grids (ie overset meshes).

The first method, called the Baseline Method here, is described visually in Figure 2. Using this method, the fringe elements are handled similarly to the interior elements. The volume integrals for the mass matrix and convective terms are integrated as normal using the local values of  $\hat{u}$ . For the flux vector, the contribution from the neighboring mesh is interpolated at the interior of the neighboring mesh's fringe element, and not its end point as is typically done. This interpolation is done using the typical finite element approach, shown in Equation (5). This method leads to stable and convergent solutions however conservation error is incurred since the contributions from the overlapping region is counted twice, once on each mesh.

Alternatively, a conservative overset approach is proposed in this work. This approach is described in Figure 3. The overall goal of the conservative overset method, is to modify both the volume and flux integrals of both fringe elements such that they each only account for a portion of the overlap region. By doing so, the elements are no longer double counting the overlap region and are analogous to a single, fully connected grid.

For the conservative overset approach, both the volume integrals and the fluxes will have to be altered. The volume integrals are modified by subtracting the integral of the cut region, as shown in Equation (9).

$$\int_a^b f(x)dx = \int_a^c f(x)dx - \int_b^c f(x)dx \quad \text{where } a < b < c \quad (9)$$

In this implementation the same number of quadrature points are used to compute both integrals, maintaining the order of accuracy for the integra-

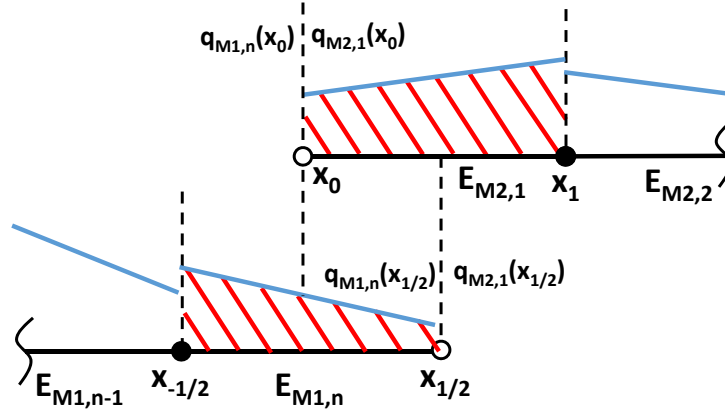


Figure 2: Schematic describing the baseline overset DG method with two meshes. Fluxes from neighboring meshes are interpolated at the element endpoints and volume integrals are calculated over the complete elements (shown in striped red)

tion. This modification is done for both the mass matrix and the convective terms. The fluxes are handled similarly to the baseline approach however instead of interpolating the neighboring flux at the end point, now it is interpolated at the point where the overlapping region is cut, called  $x_{cut}$  in Figure 3.

Note that how much of the overlap region is cut away from each mesh is up to the user to decide. For instance, both meshes can have half of the cut region removed or all of the overlapping region may be removed from one of the fringe elements while the other is left untouched. While any combination of cutting is valid, there are implications for numerical stability that will be discussed in the next section.

### 3 Numerical Stability

While conservative overset method has been shown to lead to a reduction in both L2 and conservation error (discussed below), integrating over only a portion of the element has been observed to make the mass matrix singular and ultimately lead to divergent solutions under certain circumstances. The stability of the conservative overset method depends on two main factors: the order of accuracy of the shape functions and the fraction of the element

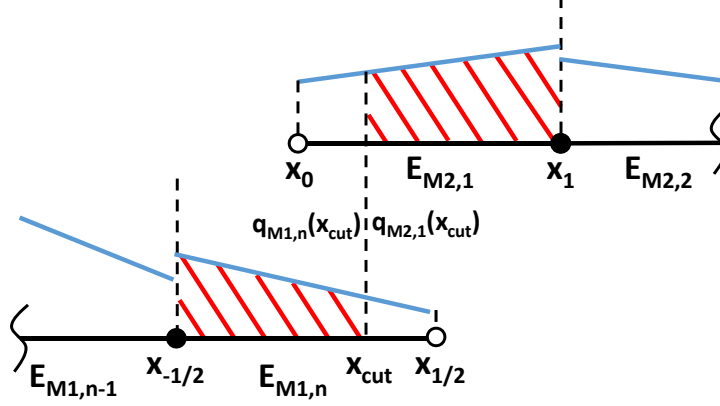


Figure 3: Schematic describing the conservative overset DG method with two meshes. Portions of the overlap region are removed from each of the volume integrals and the fluxes are calculated at the point where the overlap is split.

that is being cut.

As the spatial order of accuracy is increased, it can be observed that the complete mass matrix (i.e. over the entire element) becomes larger and more ill-conditioned as a result. This holds true for both Lagrange (nodal) and Legendre (modal) bases. This is exasperated when the mass matrix is computed over only a portion of the element. The more of the element is removed, the worse the effect is. Because of this, it has been observed that the conservative overset method fails at high orders ( $p \geq 5$ ) and when large portions of the elements have been cut away.

To combat this, additional gauss points ( $ns_{hp}+3$ ) were added and Tikhonov regularization was added to improve the condition of the mass matrix. The regularization essentially solves a similar L2 minimization problem with a higher condition number (more stable) rather than directly inverting the mass matrix. While this is a more stable approach, it comes at the cost of additional bias (and conservation error). The least amount of regularization is added ( $\lambda = 0$ ) in order to minimize the added conservation error and retain the benefits from the conservative overset. Using the additional gauss points and regularization, the stability was improved to the point that  $p=5$  simulations with 95% of the element removed remained stable. However to go beyond  $p=5$  required so much regularization that the conservation error

increased beyond baseline values.

As an aside, note that by only integrating over a portion of the element, the orthogonality of the Legendre-based mass matrix is broken. When integrating over a partial element, the mass matrix is fully populated instead of being purely diagonal, as is the case normally.

## 4 Results

The advection equation was solved on two meshes on a periodic domain. Theoretically, after a single flow through when the wave returned to its original position, the solution should be identical to the initial condition. Thus the L2 and conservation error were defined as shown in Equations (10) and (11) below.

$$e_{L2} = \left( \int_{\Omega} (u(x, T) - u(x, 0))^2 d\Omega \right)^{1/2} \quad (10)$$

$$e_{cons} = \left| \int_{\Omega} u(x, 0) d\Omega - \int_{\Omega} u(x, T) d\Omega \right| \quad (11)$$

where T is the final time. As expected, the L2 error converges at a rate of  $(p + 1)$ . The conservative oversight method shows a lower error than the baseline methods.

In the test case, the coarse mesh spanned from  $[-1, 1]$  and the fine mesh from  $[-0.268, 0.732]$ . The mesh size of the fine grid was half the size of the coarse grid for all cases. A mesh and p-refinement study was done using both the baseline and conservative oversight methods. The timestep was chosen such that a  $CFL = 0.01$  was achieved. The results are shown in Figure 4. Note that these results correspond to the case where half of the overlap region is removed from each fringe element and Legendre bases are used. The study was repeated for Lagrangian bases and very little difference was observed.

As can be seen from Figure 4, the convergence rate was maintained and follows the  $(p+1)$  curve for both the baseline and conservative oversight methods, although the conservative method led to consistently lower L2 error. For the conservation error, the baseline methods showed non-zero errors that also converged at a rate of  $(p+1)$ . On the other hand, the conservative oversight errors were consistently at or close to machine epsilon. At higher orders with coarse grids, the conservation error using the conservative method was at its maximum but was still 5 or 6 orders of magnitude smaller than that of the baseline method.

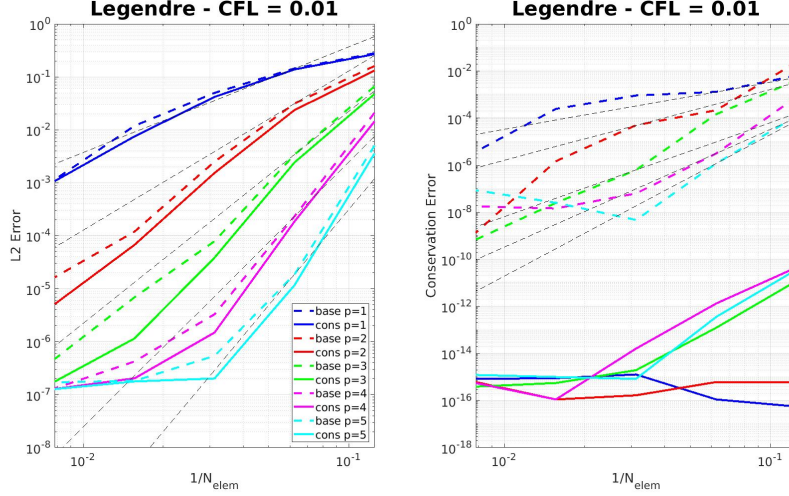


Figure 4: Convergence plots for L2 and conservation error using the baseline and conservative overset methods

The effect of the cut fraction was explored. It was found that increasing the cut fraction makes the cut mass matrix more ill conditioned. As discussed previously, this was addressed by adding in regularization in the  $Ax = b$  matrix solve at the cost of a slight increase in error. This is shown in Figure 5 which shows results for 3 cases where the fine mesh overlaps the coarse mesh by 95% of the fine mesh length. These 3 cases correspond to 1) the baseline case, 2) conservative overset where 48% of the coarse element was removed (with no regularization), and 3) conservative overset where 95% of the fine mesh was removed (with regularization). Note that without regularization, the 95% cut case diverges for  $p \geq 3$  (not shown) but with regularization it is able to remain stable until  $p=5$ . This additional stability comes at the cost of an increase in the conservation error but it is still 4+ orders of magnitude lower than the baseline case. The L2 error is unchanged.

Although this method is shown to improve stability, best practice would still be to reduce the cut length as much as possible by either removing half of the overlap from both fine and coarse elements or by removing it only from the coarse element.

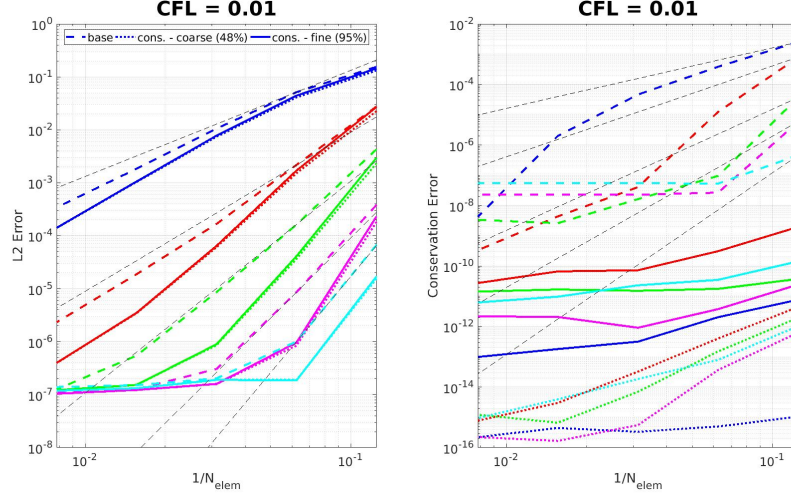


Figure 5: Convergence plots for 1) the baseline case, 2) conservative overset where 48% of the coarse element was removed, and 3) conservative overset where 95% of the fine mesh was removed

## 5 Conclusion

A conservative overset approach is described and applied to a 1D advection problem using discontinuous Galerkin finite elements. The conservative approach was shown to lead to lower L2 error as well as eliminating the conservation error. There are some stability issues with the approach, although they can be avoided by keeping the spatial order of accuracy below  $\approx 6$ . Regularization was added to improve stability in cases where there is high overlap between the elements but best practice is still to avoid this situation whenever possible.